

ESTIMATION OF NOISE OF INSTALLED TURBOFAN ENGINES

Daniel Amado Muraro, amadomuraro@gmail.com

Bento Silva de Mattos, bmattos@ita.br

Instituto Tecnológico de Aeronáutica, São José dos Campos, SP, Brazil

***Abstract.** In the present days, a lot of effort is being exercised for developing airliners with low internal and external noise signature. This is not just a trend and it is already largely widespread in the aeronautics and aviation communities of today. Noisy aircraft either can simply be banned from operating in certain airports or are subjected to higher fees for operating in many of them. In this context, the present work is concerned with the study of noise generated by aircraft powerplant and its propagation. The study of this subject resulted into a development of a numerical tool for the external noise estimation that is generated by installed turbofan engines. For the elaboration of the computational code, several methods described in some NASA TM-X reports were employed. Each of those reports addressed some specific component of the engine such as inlet, core, turbine, and nozzle. The MATLAB[®] platform was chosen to house the code under consideration. The ability of the code to correctly predict the noise signature was evaluated by the confrontation with the ESDU methodology and a similar work developed in the University of Berlin. The applications in aircraft design are exemplified and discussed in the present work.*

***Keywords:** Aeroacoustics, aircraft noise, turbofan engines*

1. INTRODUCTION

For the development of aircraft, the design team in charge evaluates several configuration candidates in the conceptual phase. Parameters such as wing airfoils, wing vertical location, tail surfaces configuration, and engine location are some of the most important ones. The final configuration is usually chosen by considering economics, fulfillment of general requirements, manufacturing costs, competitive analysis, and so on.

Requirements such as cruise altitude, maximum operational speed, and range will heavily impact on any configuration under consideration, as well as passenger capacity, range, and field performance. In order to simultaneously consider all possible variables, multi-disciplinary design optimization (MDO) frameworks are employed in the majority aircraft manufacturers of today. The aerospace disciplines are related in a conflicting and non-linear manner, which makes the optimization unavoidable. MDO requires a high degree of integration among the disciplines under consideration. Typical disciplines are aeroacoustics, aerodynamics, structure, loads, aeroelasticity, flight mechanics, costs, and other related to aircraft systems.

The main concern of this work is to develop a tool to estimate the external noise caused by turbofan engines. This tool must be computationally efficient to be used as one of the criteria for aircraft selection in MDO frameworks. A similar Undergraduation work carried out by Michael Schmid [Schmid, 2001] at the University of Berlin provided the main guidelines for the establishment of our methodology. The results obtained with the present work were compared to that from Schmid's code and to the ESDU methodology [ESDU, 1998 and 2005].

Several works have been carried out on engine noise, some of them with more accurate methods, based on CFD (computational fluid dynamics). However, they are not adequate for MDO use, because more processing time is needed. By the use of lower computational cost semi-empirical routines, the adequate precision for conceptual MDO studies is achieved.

Air traffic had a substantial increase in recent years. There are many reasons for this, among them the decrease in the tickets prices that made the aviation more accessible to everyone. The time saved in aircraft travel helped it become more popular. As a consequence, the number of transported people increased, making the takeoff and landings more frequent, and it caused the noise to become one of major problems in development and certification of new aircraft, and also in the construction of new airports. The size of the airplanes also increased to absorb this bigger demand of passengers, and bigger aircraft tend to produce more noise.

In the design of modern aircraft, the generated noise has a greater importance every day. The reason is the environmental laws that are becoming more rigorous, due to the complain of European and American cities.

Aircraft that do not meet the current noise restrictions face some problems to operate in airports with populated cities nearby. Airlines can be forced to pay taxes in some of them, or can even be prohibited to operate in others. Older aircraft are often required to use some noise reduction operational techniques (by the use of a lower thrust setting).

2. METHODOLOGY

2.1. General Methodology

Works in the National Aeronautics and Space Agency (NASA) are very diverse. For the estimation of engines noise we can highlight some NASA technical memorandum reports, which the methodology presented here is based. For every engine component there is a report that presents an estimation method. Table 1 shows the reports used for each engine component, it's author and year of publication.

Table 1. Noise estimation methodology

Component	Method	Author and Year
Fan and Compressor	NASA TM-X 71763	Heidmann, 1979
Combustion chamber	NASA TM-X 71627	Huff, 1974
Turbine	NASA TM-X 73566	Krejsa & Valerina, 1976
Exhaust Jet	NASA TM-X 71618	Stone, 1974

2.2. Fan noise prediction

The fan and compressor noise comprises a broadband spectrum, and different tones, that occur in fundamental blade passage frequency and it's harmonics. If the blade tip speed is supersonic, there is another component. The predicted free-field radiation patterns consist of a composite of the following separately predicted noise components:

- (1) Noise emitted from the fan or compressor inlet duct
 - (a) Broadband noise
 - (b) Discrete-tone noise
 - (c) Combination-tone noise
- (2) Noise emitted from the fan discharge duct
 - (a) Broadband noise
 - (b) Discrete-tone noise

The procedure involves predicting the spectrum shape, spectrum level, and freefield directivity for each of the noise components. The component spectra at any polar angle are then combined on an energy basis to form a single spectrum. The procedure is directed to single-stage fan. For two-stage fans, each stage is treated as an independent source and the sound energy produced by each stage is combined. No correction is made for blade row attenuation.

The noise generated is caused by the conversion of mechanical energy into output sound power, which is proportional to the temperature difference in the process.

For the convenience of specifying commonly used fan or compressor variables, the equivalent of power and specific work are used to normalize the levels of all the component noise sources. The product of mass flow rate \dot{m} and temperature rise ΔT is used for power. Specific work is expressed as temperature rise. Using these equivalents gives the general form of the normalized sound pressure levels as

$$SPL - 20 \log_{10} \left(\frac{\Delta T}{\Delta T_0} \right) - 10 \log_{10} \left(\frac{\dot{m}}{\dot{m}_0} \right) = f(\text{design}) \quad (1)$$

Broadband noise

The broadband noise is caused by the turbulence around the rotor/stator vanes, and in the inlet duct wall. The following relation was derived from the one third octave band spectrum analysis:

$$L = 10 \log_{10} \left(e^{\left[\frac{1}{2} \left[\frac{\ln \left(\frac{f}{2.5 * fb} \right)}{\ln(2.2)} \right]^2 \right]} \right) \quad (2)$$

Where fb is the blade passage frequency, defined by: $fb = n_{rotor} * rpm_{rotor} / 60$. n_{rotor} is the number of rotor blades, and rpm_{rotor} is the rotor revolution speed, in rpm.

The one third octave bands sound pressure level for a single fan is given by the general form of the normalized sound pressure level, added by 3 correction factors and the spectrum factor.

$$Lc = 20 \log_{10} \left(\frac{\Delta T}{\Delta T_0} \right) + 10 \log_{10} \left(\frac{r}{r_0} \right) + F_1 [M_{TR}, (M_{TR})_D] + F_2 (RSS) + F_3 (q) \quad (3)$$

Where F_1 considers the rotor-tip relative inlet Mach number, and it's design value:

$$\left. \begin{aligned} F_1 &= 58.5 & (M_{TR})_D \leq 1.0; M_{TR} \leq 0.9 \\ F_1 &= 58.5 + 20 \log_{10} (M_{TR})_D & (M_{TR})_D > 1.0; M_{TR} \leq 0.9 \\ F_1 &= 58.5 + 20 \log_{10} (M_{TR})_D - 20 \log_{10} \left(\frac{M_{TR}}{0.9} \right) & (M_{TR})_D > 1.0; M_{TR} > 0.9 \\ F_1 &= 58.5 - 20 \log_{10} \left(\frac{M_{TR}}{0.9} \right) & (M_{TR})_D \leq 1.0; M_{TR} > 0.9 \end{aligned} \right\} \quad (4)$$

F_2 considers the spacing between rotor and stator vanes, and depends on the presence of inlet flow distortions.

- Without inlet flow distortions:

$$F_2 = -5 \log_{10} \left(\frac{RSS}{300} \right) \quad (5)$$

- With inlet flow distortions:

$$\left. \begin{aligned} F_2 &= -5 \log_{10} \left(\frac{RSS}{300} \right) & \text{for } RSS \leq 100 \\ F_2 &= -5 \log_{10} \left(\frac{100}{300} \right) & \text{for } RSS > 100 \end{aligned} \right\} \quad (6)$$

F_3 considers the angle between the flight path and the direction of the propagation of sound, and is shown in Table 2 below.

Table 2: F_3 factor for broadband noise at inlet

q [°]	F_3 [dB]						
0	-2.0	30	0.0	60	-4.5	90	-15.0
10	-1.0	40	0.0	70	-7.5	100	-19.0
20	0.0	50	-2.0	80	-11.0	110	-25.0

The broadband spectrum for one third octave band is given by:

$$SPL(f) = Lc + F_4 \left(\frac{f}{fb} \right) \quad (7)$$

Where $F_4 \left(\frac{f}{fb} \right)$ is given by equation 2.

Discrete tone noise

The generation of discrete tones is caused by lift variations in rotors and stators blades. Another source can be the inlet flow turbulence.

The spectral content of the discrete tone noise depends on the presence of inlet guide vanes and also of the cutoff factor δ , which is calculated by:

$$d = \left| \frac{M_T}{1 - \frac{n_{stator}}{n_{rotor}}} \right| \quad (8)$$

The peak sound pressure level for the fundamental tone is given by the same equation of the broadband noise (eq. 3), but the factors F_1 , F_2 and F_3 have different values.

$$\left. \begin{aligned} F_1 &= 60.5 & (M_{TR})_D \leq 1.0; M_{TR} \leq 0.72 \\ F_1 &= 60.5 + 20 \log_{10} (M_{TR})_D & (M_{TR})_D > 1.0; M_{TR} \leq 0.72 \end{aligned} \right\} \quad (9)$$

For $(M_{TR})_D > 1.0; M_{TR} > 0.72$, F_1 is the least of the following expressions:

$$\left. \begin{aligned} F_1 &= 60.5 + 20 \log_{10} (M_{TR})_D + 50 \log_{10} \left(\frac{M_{TR}}{0.72} \right) \\ F_1 &= 58.5 + 80 \log_{10} \left(\frac{(M_{TR})_D}{M_{TR}} \right) \end{aligned} \right\} \quad (10)$$

F_2 is two times the value of the same broadband factor.

- Without inlet flow distortions:

$$F_2 = -10 \log_{10} \left(\frac{RSS}{300} \right) \quad (11)$$

- With inlet flow distortions:

$$\left. \begin{aligned} F_2 &= -10 \log_{10} \left(\frac{RSS}{300} \right) & \text{for } RSS \leq 100 \\ F_2 &= -10 \log_{10} \left(\frac{100}{300} \right) & \text{for } RSS > 100 \end{aligned} \right\} \quad (12)$$

F_3 is given by:

Table 3: F_3 factor for discrete tone noise at inlet

q [°]	F_3 [dB]						
0	-3.0	30	0.0	60	-3.5	90	-14.5
10	-1.5	40	0.0	70	-6.8	100	-19.0
20	0.0	50	-1.2	80	-10.5		

The sound pressure level for the discrete tone harmonics is obtained by an energy sum of the rotor/stator interaction tone levels, and the inlet flow distortions tone levels, if applicable.

$$SPL(f) = Lc + 10 \log_{10} \left(10^{0.1 F_4 \left(\frac{f}{f_b} \right)} + 10^{0.1 F_5 \left(\frac{f}{f_b} \right)} \right) \quad (13)$$

F_4 depends on the presence of inlet guide vanes:

With inlet guide vanes:

$$\left. \begin{aligned} F_4 &= 0 & \text{for } k=1 \text{ e } d > 1,05 \\ F_4 &= -3 - 3k & \text{for } k \geq 2 \text{ e } d > 1,05 \\ F_4 &= -8 & \text{for } k=1 \text{ e } d \leq 1,05 \\ F_4 &= -3 - 3k & \text{for } k \geq 2 \text{ e } d \leq 1,05 \end{aligned} \right\} \quad (14)$$

Without inlet guide vanes:

$$\left. \begin{aligned} F_4 &= 3 - 3k & \text{for } d > 1,05 \\ F_4 &= -8 & \text{for } k=1 \text{ e } d \leq 1,05 \\ F_4 &= 3 - 3k & \text{for } k \geq 2 \text{ e } d \leq 1,05 \end{aligned} \right\} \quad (15)$$

F_5 considers the presence of inlet flow distortions, and falls 10 dB for each harmonic order, as in the equation 16. Without inlet flow distortions, F_5 should be neglected.

$$F_5 = 10 - 10k \quad (16)$$

Combination tone noise

The combination tone noise is present only in supersonic rotor tip speeds. It is caused by the shock waves that propagate upstream in the flow and outside of the air inlet.

The peak levels for one half, one fourth and one eighth of the blade passage frequency is:

$$Lc = 20 \log_{10} \left(\frac{\Delta T}{\Delta T_0} \right) + 10 \log_{10} \left(\frac{r_{\text{tip}}}{r_{\text{hub}}} \right) + F_1[M_{TR}] + F_2(q) + C \quad (17)$$

F_1 is calculated by:

$$\left. \begin{aligned} f/fb = 1/2 \rightarrow F_1 &= 318.49 * M_{TR} - 288.49; M_{TR} \leq 1.146 \\ &F_1 = -14.05 * M_{TR} + 92.60; M_{TR} > 1.146 \\ f/fb = 1/4 \rightarrow F_1 &= 147.52 * M_{TR} - 117.52; M_{TR} \leq 1.322 \\ &F_1 = -13.27 * M_{TR} + 95.05; M_{TR} > 1.322 \\ f/fb = 1/8 \rightarrow F_1 &= 67.54 * M_{TR} - 37.54; M_{TR} \leq 1.610 \\ &F_1 = -12.05 * M_{TR} + 90.60; M_{TR} > 1.610 \end{aligned} \right\} \quad (18)$$

F_2 is given by:

Table 4: F_2 factor for combination tone noise

q [°]	F_2 [dB]						
0	-9.5	50	0.0	100	-9.5	150	-12.0
10	-8.5	60	0.0	110	-10.0	160	-12.5
20	-7.0	70	-3.5	120	-10.5	170	-13.0
30	-5.0	80	-7.5	130	-11.0	180	-13.5
40	-2.0	90	-9.0	140	-11.5		

C equals -5 dB if the fan has inlet guide vanes and 0 dB otherwise.

The sound pressure level spectrum for the 3 sub-components is:

$$SPL(f) = Lc + F_3 \left(\frac{f}{f_b} \right) \quad (19)$$

F_3 is given by 3 curves that peaks at one half, one fourth and one eighth of the blade passage frequency.

$$f/fb = 1/2 \rightarrow F_3 = 30 \log_{10} \left(2 \frac{f}{f_b} \right); \frac{f}{f_b} \leq \frac{1}{2} \quad (20)$$

$$F_3 = -30 \log_{10} \left(2 \frac{f}{f_b} \right); \frac{f}{f_b} > \frac{1}{2}$$

$$f/fb = 1/4 \rightarrow F_3 = 50 \log_{10} \left(4 \frac{f}{f_b} \right); \frac{f}{f_b} \leq \frac{1}{4} \quad (21)$$

$$F_3 = -50 \log_{10} \left(4 \frac{f}{f_b} \right); \frac{f}{f_b} > \frac{1}{4}$$

$$f/fb = 1/8 \rightarrow F_3 = 50 \log_{10} \left(8 \frac{f}{f_b} \right); \frac{f}{f_b} \leq \frac{1}{8} \quad (22)$$

$$F_3 = -30 \log_{10} \left(8 \frac{f}{f_b} \right); \frac{f}{f_b} > \frac{1}{8}$$

The combination tone noise is obtained as an energy sum of the 3 components spectra.

Fan Exhaust Duct

Broadband noise

The broadband noise is determined the same way as for the inlet duct, but it considers a correction for the presence of inlet guide vanes. It's equation is:

$$L_c = 20 \log_{10} \left(\frac{\Delta T}{\Delta T_0} \right) + 10 \log_{10} \left(\frac{r_{\text{in}}}{r_{\text{in}_0}} \right) + F_1 [M_{TR}, (M_{TR})_D] + F_2 (RSS) + F_3 (q) \quad (23)$$

With F_1 given by:

$$\left. \begin{aligned} F_1 &= 60.0 && (M_{TR})_D \leq 1.0; M_{TR} \leq 1.0 \\ F_1 &= 60.0 + 20 \log_{10} (M_{TR})_D && (M_{TR})_D > 1.0; M_{TR} \leq 1.0 \\ F_1 &= 60.0 + 20 \log_{10} (M_{TR})_D - 20 \log_{10} (M_{TR}) && (M_{TR})_D > 1.0; M_{TR} > 1.0 \end{aligned} \right\} \quad (24)$$

F_2 is the same of the inlet duct, and is calculated by equations 5 and 6.

F_3 is given by:

Table 5: F_3 factor for broadband noise at discharge

q [°]	F_3 [dB]						
60	-15.8	100	-2.7	140	-2.0	180	-20.0
70	-11.5	110	-1.2	150	-6.0		
80	-8.0	120	-0.3	160	-10.0		
90	-5.0	130	0.0	170	-15.0		

The spectrum is calculated the same way as for the inlet, by the use of equation 7.

Discrete tone noise

The calculation is the same as for the inlet duct, but considering a factor that accounts for the presence of inlet guide vanes. Equation 23 can be used, but with different factor for F_1 , F_2 and F_3 .

$$\left. \begin{aligned} F_1 &= 63.0 && (M_{TR})_D \leq 1.0; M_{TR} \leq 1.0 \\ F_1 &= 63.0 + 20 \log_{10} (M_{TR})_D && (M_{TR})_D > 1.0; M_{TR} \leq 1.0 \\ F_1 &= 63.0 + 20 \log_{10} (M_{TR})_D - 20 \log_{10} (M_{TR}) && (M_{TR})_D > 1.0; M_{TR} > 1.0 \end{aligned} \right\} \quad (25)$$

F_2 is the same of the inlet duct, and is calculated by equations 11 and 12.

F_3 is given by:

Table 6: F_3 factor for discrete tone noise at discharge

q [°]	F_3 [dB]			q [°]	F_3 [dB]	q [°]	F_3 [dB]
60	-15.0	100	-3.0	140	-2.0	180	-18.0
70	-11.0	110	-1.0	150	-5.5		
80	-8.0	120	0.0	160	-9.0		
90	-5.0	130	0.0	170	-13.0		

The spectrum can be calculated by equation 7, with $F_4 \left(\frac{f}{fb} \right)$ calculated by equations 14 or 15.

2.3 Combustion chamber noise prediction

The combustion chamber noise is caused by a series of factors, among the combustion process, the flux by internal obstructions, and the friction on the duct walls. It is mostly a broadband and low-frequency noise. It is related to the jet noise, and some methods estimate the combustion chamber noise considering it proportional to the jet noise. The method used here follows another direction, estimating the noise by engine parameters.

Calculation procedure

For the noise estimation, the overall sound power level will be calculated, because it is simpler than the overall sound pressure level. An general equation for it is given as follows:

$$OAPWL = 56.5 + 10 \log_{10} \left[\frac{\dot{m}_{chamber} (T_{exit} - T_{entry}) \frac{P_{entry}}{P_0} \frac{T_0}{T_{entry}}}{0.4536} \right] \quad (26)$$

In order to determine the sound pressure level, the angle of directivity and the distance are considered with the following equation.

$$OASPL_{q,r} = OAPWL + (OASPL_q - OAPWL) - 20 \log_{10} \left(\frac{r}{3.28} \right) \quad (27)$$

The factor $OASPL_q - OAPWL$ is a function of the directivity angle

Table 7: $OASPL_q - OAPWL$ factor for combustion chamber noise

q [°]	$OASPL_q - OAPWL$ [dB]	q [°]	$OASPL_q - OAPWL$ [dB]
0	-32.4	100	-19.6
10	-30.8	110	-18.8
20	-29.6	120	-18.6
30	-28.0	130	-18.5
40	-26.6	140	-18.7
50	-25.0	150	-19.0
60	-24.0	160	-19.0
70	-23.4	170	-19.1
80	-22.3	180	-19.2
90	-20.8		

The spectrum content is assumed to be the same as for the jet noise, and is given by:

$$SPL_{q,f,r} = OASPL_{q,r} + (SPL - OASPL)_q \quad (28)$$

The peak frequency f_p can be considered to be 400 Hz, and the factor $(SPL - OASPL)_q$ can be obtained by the development in Fourier series.

For $f \leq f_p$:

$$\begin{aligned} SPL_f - OASPL_q = & 15.02 \left(\log_{10} \frac{f}{f_p} \right)^6 + 65.92 \left(\log_{10} \frac{f}{f_p} \right)^5 + 108.33 \left(\log_{10} \frac{f}{f_p} \right)^4 \\ & + 75.37 \left(\log_{10} \frac{f}{f_p} \right)^3 + 2.96 \left(\log_{10} \frac{f}{f_p} \right)^2 + 1.48 \left(\log_{10} \frac{f}{f_p} \right) - 10 \end{aligned} \quad (29)$$

For $f > f_p$:

$$\begin{aligned} SPL_f - OASPL_q = & 0.20 \left(\log_{10} \frac{f}{f_p} \right)^6 - 1.02 \left(\log_{10} \frac{f}{f_p} \right)^5 + 1.21 \left(\log_{10} \frac{f}{f_p} \right)^4 \\ & + 2.72 \left(\log_{10} \frac{f}{f_p} \right)^3 - 11.54 \left(\log_{10} \frac{f}{f_p} \right)^2 - 1.30 \left(\log_{10} \frac{f}{f_p} \right) - 10 \end{aligned} \quad (30)$$

2.4 Turbine noise prediction

As in the fan noise, the turbine noise is characterized by a broadband spectrum, caused by the random lift fluctuations in rotors and stators blades, and discrete tone noises, caused by the cyclic interaction of the airflow between them.

The prediction method described here determines the noise at a 45.7 m (150 ft) radial distance from the noise source, and must be corrected to a 1 m radius by the sum of the atmospheric damping.

Broadband noise

The following relation can be used for the calculation of the one third octave band broadband noise peak level.

$$SPL_{peak} = 10 \log_{10} \left[\left(\frac{V_{TR} \cdot V_{soundref}}{V_R \cdot V_{sound}} \right)^3 \left(\frac{r_{turbine}}{r_R} \right) (1 - M_0 \cdot \cos \alpha)^{-4} \right] + F_1(q) - 10 \quad (31)$$

F_1 considers the angle between the flight path and the propagation of sound. It's value is show below, together with the factor F_3 .

Table 8: F_1 and F_3 factors for turbine noise

Angle	Broadband noise	Discrete tone noise	Angle	Broadband noise	Discrete tone noise
q [°]	F_1 [dB]	F_3 [dB]	q [°]	F_1 [dB]	F_3 [dB]
40	-21	-27	110	0	0
50	-17	-21.7	120	-1.4	-2.1
60	-13	-18	130	-5	-8
70	-10	-14	140	-9	-14
80	-7	-10	150	-14	-20
90	-4	-5.5	160	-19	-26
100	-1.2	-2.3			

The sound spectrum can then be calculated as:

$$SPL_{broadband} = SPL_{peak} + F_2 \left(\frac{f}{f_0} \right) \quad (32)$$

f_0 is the fundamental frequency, and is calculated the same way as the fan noise fundamental frequency, but considering the Doppler effect.

$$f_0 = \frac{n_{rotorturbine} \cdot rpm_{turbine}}{60(1 - M_0 \cdot \cos \alpha)} \quad (33)$$

$$F_2 = +10 \log_{10} \frac{f}{f_0} \quad \text{for} \quad f < f_0 \quad (34)$$

$$F_2 = -20 \log_{10} \frac{f}{f_0} \quad \text{for} \quad f > f_0$$

Discrete tone noise

The turbine discrete tone noise component is defined in a similar matter as the broadband noise. The sound pressure level for the first harmonic order, at 45.7 m is:

$$SPL_{tone} = 10 \log_{10} \left[\left(\frac{V_{TR}}{V_R} \right)^{0.6} \left(\frac{V_{soundref}}{V_{sound}} \right)^3 \left(\frac{r_{turbine}}{r_R} \right) \left(\frac{RSS}{100\%} \right) (1 - M_0 \cdot \cos \alpha)^{-4} \right] + F_3(q) + 56 \quad (35)$$

The factor F_3 also depends on the directivity angle, and was already defined.

For each subsequent harmonic order, the sound pressure level has a 10 dB decrease.

2.5 Jet noise prediction

The jet noise is caused by the mixing of the cold and cold air flux with the atmosphere, being directly proportional to the jet velocity. The following relation express this dependence:

$$P = k \frac{r_{jet}}{r_{amb}} A \frac{V^8}{V_{sound}^5} \quad (36)$$

The noise also depends on the jet temperature. In low velocities, the increase in jet temperatures tends to increase the generated noise, although in high velocities the opposite effect is observed. The directivity angle also affects the noise

due to convectivity effects, and since it's effects are lower at an angle $\theta=90^\circ$, this angle was chosen as a baseline for prediction. The flight velocity is another factor, the noise at the rear of the engine is decreased and the noise ahead of it is increased when the airplane flies faster.

In order to improve the mixing in a turbofan engine and consequently reduces the noise, a lot of effort has been concentrated in the design of more efficient nozzles.

Prediction method

The approach taken is described briefly as follows:

1) The overall sound pressure level at $\theta=90^\circ$, in normalized form, is first predicted as a function of jet velocity and other pertinent variables.

2) The normalized sound pressure level spectrum is then predicted at $\theta = 90^\circ$.

3) Then the directivity in normalized 1/3-octave bands is considered, and the spectra at various angles obtained.

The prediction is first developed for single, circular nozzles, starting with shock-free jets having no ambient velocity. The effects of shock noise and forward velocity are then considered, and the method is extended to plug nozzles and coaxial nozzles.

Circular nozzles

The overall sound pressure level at $\theta=90^\circ$, $OASPL_{90^\circ}$, is first determined by the following equation

$$OASPL_{90^\circ} - 10 \log_{10} \left[\frac{A_{jet}}{r^2} \left(\frac{r_{amb}}{r_{ISA}} \right)^2 \left(\frac{V_{sound}}{V_{soundISA}} \right)^4 \right] - 10 * w * \log_{10} \left(\frac{r_{jet}}{r_{amb}} \right) = 141 + 10 \log_{10} \left[\frac{(V_{jet}/V_{sound})^{7.5}}{1 + 0.01 * (V_{jet}/V_{sound})^{4.5}} \right] \quad (37)$$

Where w is equal to:

$$w = \frac{3 \left(\frac{V_{jet}}{V_{sound}} \right)^{3.5}}{0.60 + \left(\frac{V_{jet}}{V_{sound}} \right)^{3.5}} - 1 \quad (38)$$

The frequency is represented by a nondimensional frequency parameter, the Strouhal number, which is defined as:

$$S = \left(\frac{f * D_e}{V_{jet}} \right) \left(\frac{T_{jet}}{T_{amb}} \right)^{0.4} \quad (39)$$

The effect of source convection on sound directivity is then considered by the introduction of a factor $\left[\frac{1 + (M_c * \cos(q))}{\sqrt[3]{1 + M_c^5}} \right]^{-3}$ in the sound pressure level calculation. Figure 1 shows the recommended prediction curves for

SPL spectra. The ordinate is $SPL - OASPL_{90^\circ} + 30 \log_{10} \left[\frac{1 + M_c * \cos(q)}{\sqrt[3]{1 + M_c^5}} \right]$, and the abscissa is a modified Strouhal

number defined by

$$S = \left(\frac{f * D_e}{V_{jet}} \right) \left(\frac{T_{jet}}{T_{amb}} \right)^{0.4(1 + \cos(q'))} \quad (40)$$

Where $q' = q \left(\frac{V_{jet}}{V_{sound}} \right)^{0.1}$

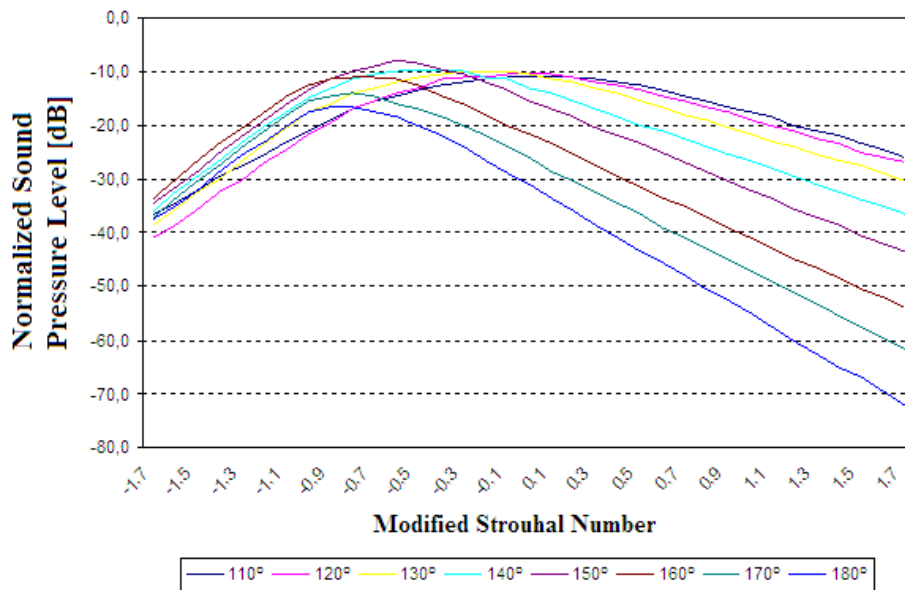


Figure 1: Recommended prediction curves for shock-free jet noise sound pressure level spectra

The effects of forward velocity are then considered. At $\theta=90^\circ$ there is no Doppler effect, and the velocity dependence can be incorporated in equation 37 by the replacement of V_{jet} with $V_{jet} \left(1 - \frac{V_{amb}}{V_{jet}}\right)^{\frac{3}{4}}$. The equation then becomes:

$$OASPL_{90^\circ} - 10 \log_{10} \left[\frac{A_{jet}}{r^2} \left(\frac{r_{amb}}{r_{ISA}} \right)^2 \left(\frac{V_{sound}}{V_{soundISA}} \right)^4 \right] - 10 \left[\frac{3 \left(\left(\frac{V_{jet}}{V_{sound}} \right) \left(1 - \frac{V_{sound}}{V_{jet}} \right)^{\frac{3}{4}} \right)^{\frac{3}{5}}}{0.60 + \left(\frac{V_{jet}}{V_{sound}} \left(1 - \frac{V_{amb}}{V_{jet}} \right)^{\frac{3}{4}} \right)^{\frac{3}{5}}} - 1 \right]^* \quad (41)$$

$$\log_{10} \left(\frac{r_{jet}}{r_{amb}} \right) = 141 + 10 \log_{10} \left[\frac{\left(\frac{V_{jet}}{V_{sound}} \left(1 - \frac{V_{amb}}{V_{jet}} \right)^{\frac{3}{4}} \right)^{7.5}}{1 + 0.01 \left(\frac{V_{jet}}{V_{sound}} \left(1 - \frac{V_{amb}}{V_{jet}} \right)^{\frac{3}{4}} \right)^{4.5}} \right]$$

To include the effects of the nozzle motion, the Strouhal number is Doppler shifted:

$$S = \left(\frac{f * De}{V_{jet}} \right) \frac{(T_{jet}/T_{amb})^{0.4*(1+\cos(q'))}}{(1 + (V_{amb}/V_{sound}) \cos(q))} \quad (42)$$

The effect of motion on levels is included in the directivity plots of Figure 1 by basing the convection Mach number on relative velocity:

$$Mc = 0.62 * \frac{(V_{jet} - V_{amb})}{V_{sound}} \quad (43)$$

Plug Nozzles

Plug nozzles are sometimes used with circular nozzles, and they have a slightly lower noise levels than a circular nozzle of the same cross-sectional flow area. This is because a tapered plug could help decelerate the exhaust jet with reduced shear between the jet and the surrounding air, with a corresponding reduction in noise. To predict jet noise for a plug nozzle, equation 41 must be modified to include it's effects, by the addition of a $3 \log_{10} \left(0.10 + 2 \frac{h}{D} \right)$ factor. The equation becomes:

$$\begin{aligned}
 OASPL_{90^0} - 10 \log_{10} \left[\frac{A_{jet}}{r^2} \left(\frac{r_{amb}}{r_{ISA}} \right)^2 \left(\frac{V_{sound}}{V_{soundISA}} \right)^4 \right] - 10 \log_{10} \left[\frac{3 \left(\left(\frac{V_{jet}}{V_{sound}} \right) \left(1 - \frac{V_{sound}}{V_{jet}} \right) \right)^{\frac{3}{4}} \sqrt[3]{\frac{3}{5}}}{0.60 + \left(\left(\frac{V_{jet}}{V_{sound}} \right) \left(1 - \frac{V_{amb}}{V_{jet}} \right) \right)^{\frac{3}{4}} \sqrt[3]{\frac{3}{5}}} - 1 \right] * \\
 \log_{10} \left(\frac{r_{jet}}{r_{amb}} \right) = 141 + 3 \log_{10} \left(0.1 + 2 \frac{h}{D} \right) + 10 \log_{10} \left[\frac{\left(\frac{V_{jet}}{V_{sound}} \left(1 - \frac{V_{amb}}{V_{jet}} \right) \right)^{\frac{3}{4}} 7.5}{1 + 0.01 \left(\frac{V_{jet}}{V_{sound}} \left(1 - \frac{V_{amb}}{V_{jet}} \right) \right)^{\frac{3}{4}} 4.5} \right]
 \end{aligned} \tag{44}$$

The plug effects on the SPL spectra can be accounted for by multiplying the frequency by $\left(\frac{Dh}{De} \right)^{0.4}$ in the Strouhal number S . the curves on Figure 1 should then be used with S redefined as follows:

$$S = \frac{f * De \left(\frac{Dh}{De} \right)^{0.4} \left(\frac{T_{jet}}{T_{amb}} \right)^{0.4 * (1 + \cos(q))}}{V_{jet} \left(1 + \left(\frac{V_{jet}}{V_{sound}} \right) \cos(q) \right)} \tag{45}$$

Coaxial Nozzles

Coaxial nozzles are used in short-ducted turbofan engines, where the cold flux and hot flux are not mixed in the discharge duct. The applet considers this type of nozzle

The effects of areas, velocities and temperature ratios can increase or decrease the noise of the core jet alone, and they can be computed by equation 46 below.

$$OASPL_{90^0} - OASPL_{90^0,1} = 5 \log_{10} \left(\frac{T_{jet}}{T_{bypass}} \right) + 10 \log_{10} \left[\left(1 - \frac{V_{jet}}{V_{bypass}} \right)^m + 1,2 \frac{\left(1 + \frac{A_{bypass} \cdot V_{bypass}^2}{A_{jet} \cdot V_{jet}^2} \right)^4}{\left(1 + \frac{A_{bypass}}{A_{jet}} \right)^3} \right] \tag{46}$$

The factor m is obtained by the following expression:

$$\left. \begin{aligned}
 m &= 1.1 \sqrt{\frac{A_{bypass}}{A_{jet}}} \quad \text{for } \frac{A_{bypass}}{A_{jet}} < 29.7 \\
 m &= 6.0 \quad \text{for } \frac{A_{bypass}}{A_{jet}} \geq 29.7
 \end{aligned} \right\} \tag{47}$$

The curves of the SPL spectra are the same as a circular nozzle, but with the frequencies shifted. Figure 2 shows the frequency shift parameter as a function of the Area Ration Parameter, for 5 relative velocities $\frac{V_{bypass}}{V_{jet}}$. The Frequency

Shift Parameter F_s is defined by:

$$F_s = \left(1 - \frac{S_1}{S} \right) \left(\frac{T_{jet}}{T_{bypass}} \right) \tag{48}$$

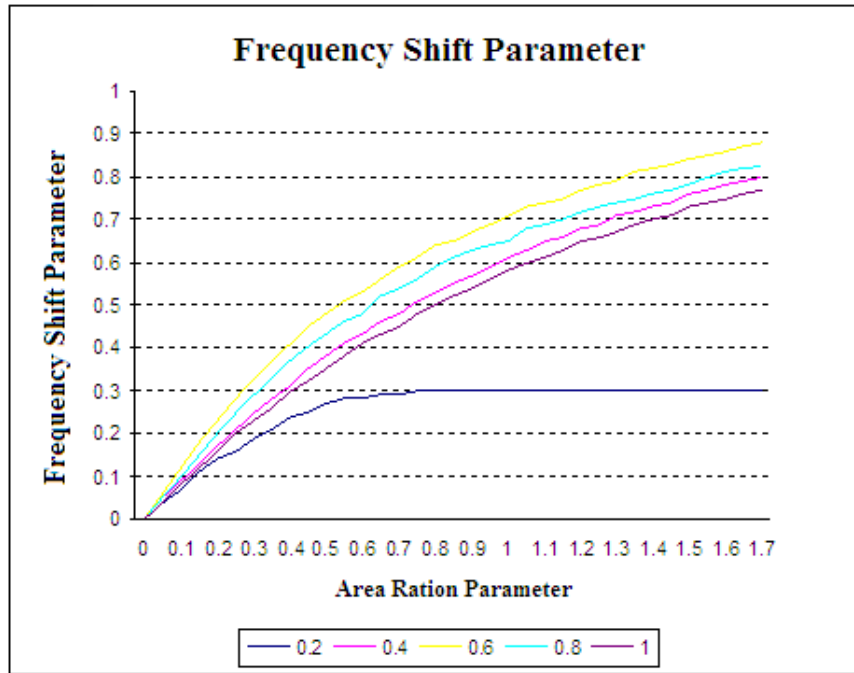


Figure 2: Frequency shift parameter

The Area Ration Parameter is defined by:

$$Area\ Ration\ Parameter = \log_{10} \left(1 + \frac{A_{bypass}}{A_{core}} \right) \quad (49)$$

3. RESULTS

3.1 General parameters

The following data is considered for comparison with the applet results, and are assumed to be the same for all engine components.

Table 9: General parameters for noise estimation methods comparison

Parameter	Value	Unit	Meaning
ΔT_{ISA}	0	°C	Temperature variation in comparison to ISA
H	0	m	Altitude
P_0	101,325	Pa	Ambient static pressure
r_0	1.225	kg/m ³	Ambient density
V_0	87	m/s	Ambient velocity or flight velocity
M_0	0.26	-	Ambient Mach number or flight Mach number
q	50	graus	Directivity angle
f_f	0	graus	Azimuth angle
r	538	m	Distance between the source and the observer

3.2 Fan noise

The following engine parameters are considered for comparison with the applet results for the fan noise.

Table 10: Engine parameters for fan noise comparison

Parameter	Value	Unit	Meaning
\dot{m}_{fan}	385	kg/s	Fan mass flow rate
PR_{fan}	1.53	-	Fan pressure ratio
h_{fan}	0.9	-	Fan efficiency
D_{fan}	1.6	m	Fan diameter
rpm_{fan}	5,233	rpm	Fan revolutions per minute
$(M_{TR})_D$	1.17	-	M_{TR} value in the fan design point
n_{rotor}	22	-	Number of fan rotor blades
n_{stator}	50	-	Number of fan stator blades
RSS	200	%	Fan rotor/stator spacing

Additionally, there must be informed if the engine has inlet guide vanes, and if there are inlet flow distortions
 The program results are shown in Figure 3, together with the results from the applet and from the ESDU methodology for comparison. The ESDU results are plotted two times, one with the original ESDU method, and another with the Heidmann method, the same used in the NASA report.

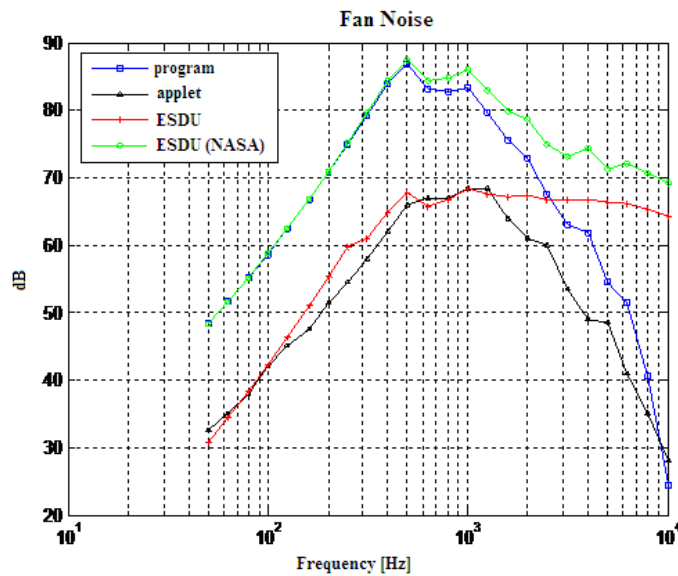


Figure 3: Comparison between the fan noise generated by the program, by the applet, and by the ESDU

We can see that the program results are very similar to the ones obtained by the ESDU results with NASA method. The difference at higher frequencies is due to the atmospheric damping, which is not considered in the ESDU method.

However, the applet results are very lower than the program's. This is probably because the applet uses the ESDU own methodology. The difference at higher frequencies is again due to the atmospheric damping.

3.3 Combustion chamber noise

There are 4 parameters needed for the noise prediction at the combustion chamber:

Table 11: Engine parameters for combustion chamber noise comparison

Parameter	Value	Unit	Meaning
$\dot{m}_{chamber}$	157	kg/s	Chamber mass flow rate
$T_{entrance}$	844	°C	Air temperature at chamber entrance
T_{exit}	1,676	°C	Air temperature at chamber exit
$P_{entrance}$	3,000,000	Pa	Air pressure at chamber entrance

The results for the program are show in Figure 4, together with the results from the applet and from the ESDU.

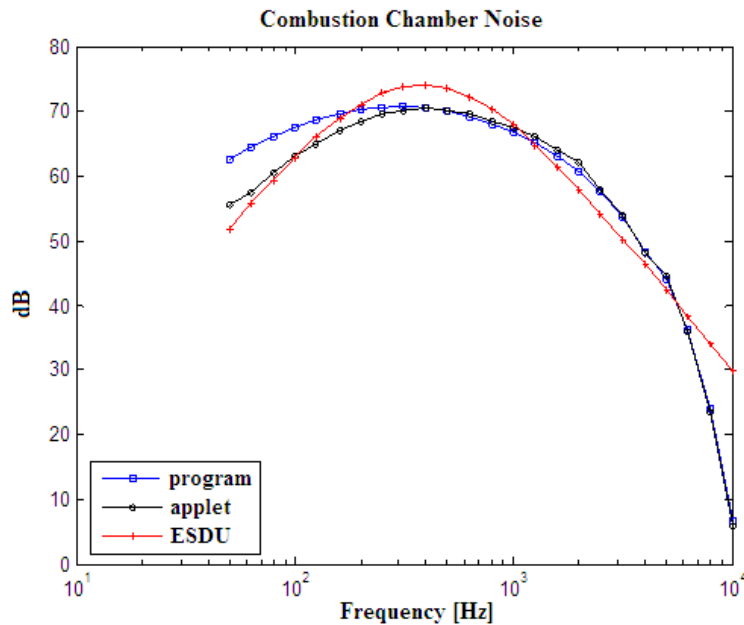


Figure 4: Comparison between the combustion chamber noise results obtained by the program, the applet, and the ESDU

The program results are very close to the applet results, and only show some difference in lower frequencies. The ESDU results are also very similar to the program's, however, since the ESDU method considers a $10 \cdot \log_{10} \left(\frac{r_0 c_0 W_{ref}}{4p \cdot p_{ref}^2} \right)$ factor, that is equal to -10.8 dB at the simulation conditions, the results are actually lower, and the ESDU plot in Figure 4 has this factor value added.

3.4 Turbine noise

For the turbine noise estimation, the following parameters are needed:

Table 12: Engine parameters for turbine noise comparison

Parameter	Value	Unit	Meaning
$\dot{m}_{turbine}$	157	kg/s	Turbine mass flow rate
$rpm_{turbine}$	5,233	rpm	Turbine revolutions per minute
$M_{TR turbine}$	0.5	-	Mach number at turbine tip
$n_{rotor turbine}$	50	-	Number of turbine rotor blades
$RSS_{turbine}$	50	%	Turbine rotor/stator spacing

The program results are show in Figure 5 below, together with the applet results for comparison. As it can be seen, both graphics are very close, showing that the program has a good correspondence.

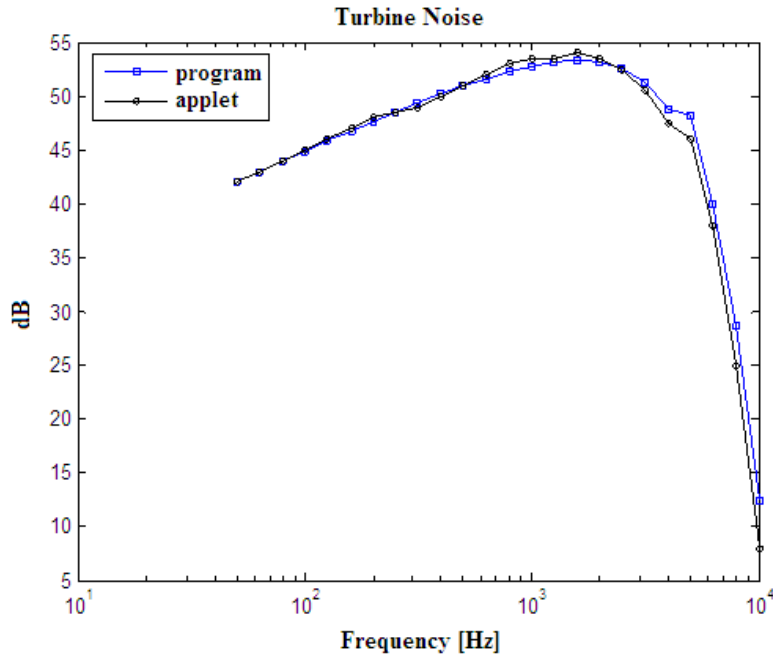


Figure 5: Comparison between the turbine noise results obtained by the program and the applet

3.5 Jet noise

For the estimation of the last part of the engine noise, various velocities, densities, areas and temperatures are needed.

Table 13: Engine parameters for jet noise comparison

Parameter	Value	Unit	Meaning
A_{jet}	0.85	m ²	Jet area
h_{gap}	0.15	m	Gap distance
A_{bypass}	2.399	m ²	Bypass area
V_{jet}	447	m/s	Jet velocity
V_{bypass}	298	m/s	Bypass velocity
T_{jet}	786	°C	Jet temperature
T_{bypass}	88	°C	Bypass temperature
r_{jet}	0.22	kg/m ³	Jet density
r_{bypass}	0.976	kg/m ³	Bypass density

Additionally, it is necessary to inform if the nozzle is circular or plug. The results for the applet and for the program with circular nozzle are show in Figure 6, while Figure 7 shows the results with plug nozzle. In the two situations the program has very good results compared to the applet, although with the plug nozzle a small difference can be seen in lower frequencies.

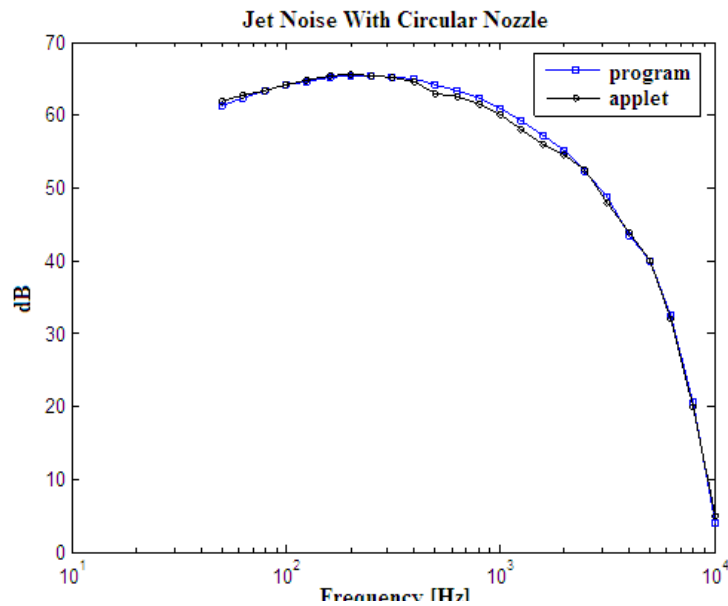


Figure 6: Comparison between the jet noise results with circular nozzles obtained by the program and the applet

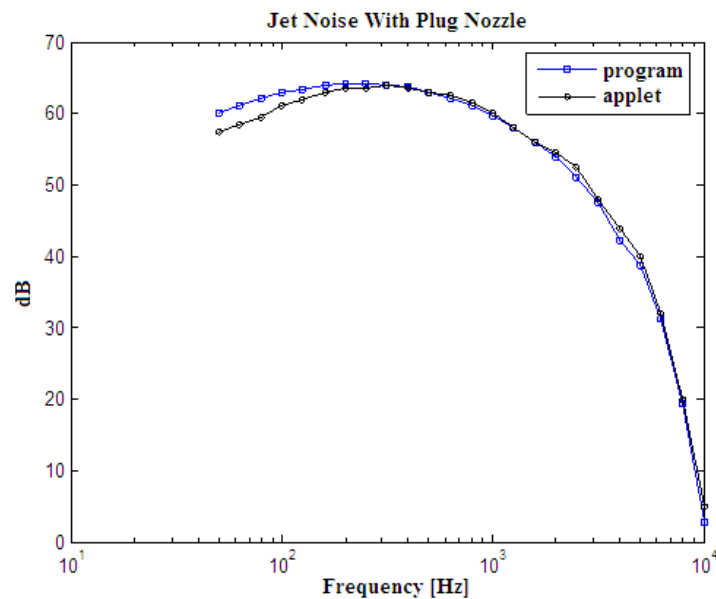


Figure 7 Comparison between the jet noise results with plug nozzles obtained by the program and the applet

4. CONCLUDING REMARKS

This work presented and implemented an external noise calculation methodology, generated by turbofan engines aircraft installed. The methodology is the same described in various NASA TM-X reports, and it was also used in an undergraduate final work of the Aeronautics and Space Institute of the Berlin Technical University. The results are analogous to the implementation made by Berlin University, and it is only necessary to check the difference between the program and the applet results, as well as both ESDU methodologies in the case of the fan noise. The most important contribution of the present work was to permit the use of a noise prediction routine in a multidisciplinary design optimization (MDO) platform.

5. REFERENCES:

- AMBEKAR, A. G. **Mechanical Vibrations and Noise Engineering**, 2006
- DUNN, D. G. & PEART, N. A. **Aircraft Noise Source and Contour Estimation**. (D6-60233, Boeing Commercial Airplane Co., NAS2-6969) NASA CR-114649, 1973
- ESDU. Engineering Science Data Unit. **Prediction of noise generated by fans and compressors in turbojet and turbofan engines**. : ESDU, 1998. (ESDU Data Item 98008).

- ESDU. Engineering Science Data Unit. **Computer-based estimation procedure for single-stream jet noise. Including far-field, static jet mixing noise database for circular nozzles**: ESDU, 1998. (ESDU Data Item 98019).
- ESDU. Engineering Science Data Unit. **An introduction to aircraft noise**: ESDU, 2002. (ESDU Data Item 02020).
- ESDU. Engineering Science Data Unit. **Prediction of combustor noise from gas turbine engines.** : ESDU, 2005. (ESDU Data Item 05001).
- FLUENT INC. **Fluent 6 for Acoustics Modeling**, 2005
- FFOWCS WILLIAMS, J. E. **Some Thoughts on the Effects of Aircraft Motion and Eddy Convection on the Noise from Air Jet**: USAA Rept. 155 Southhampton Univ. 1960
- FFOWCS WILLIAMS, J. E. **The Noise From Turbulence Convected at High Speed**. PhiloTrans. Roy. Soc. ,London, ser. A, vol. 255, no. 1061, 1963
- FOLMER-JOHNSON, T. N. O. **Acústica**, 1968
- GERGES, SAMIR N. Y. **Ruído – Fundamentos e Controle**. 2.ed. Florianópolis, SC: NR Editora, 2000.
- GOLDSTEIN. M. E. & HOWES, W. L. **New Aspects of Subsonic Aerodynamic Noise Theory**, NASA TN D-7158, 1973
- HASSALL, J. R. & ZAVERI K. **Acoustic Noise Measurement**, 1979
- HEIDMANN, M. F. **NASA TM X-71763 Interim Prediction Method for Fan and Compressor Noise**, 1979
- HUFF, D. **Technologies for Turbofan Noise Reduction**, NASA Glenn Research Center, 2004
- HUFF, R. G.; CLARK, B. J. & DORSCH, R. G. **NASA TM X-71627 Interim Prediction Method for Low Frequency Core Engine Noise**, 1974
- HUNTER, JOSEPH L. **Acoustics**, New Jersey, 1957
- KINSLER, L. E. **Fundamentals of Acoustics**, 1950
- KREJSA, E. A. & VALERINA, M. F. **NASA TM X-73566 Interim Prediction Method for Turbine Noise**, 1976
- LIGHTHILL, M. J. **On Sound Generated Aerodynamic part I General Theory**, 1952
- LIGHTHILL, M. J. **On Sound Generated Aerodynamic part II Turbulence as a Source of Sound**, 1952
- MOTSINGER, R. **Prediction of Engine Combustor Noise and Correlation with T64 Engine Low Frequency Noise**. R72AEG313, General Electric Co., 1972
- MURARO, D. A. **Estimação de Ruído de Motores Turbofan Instalados em Aeronaves de Transporte**. Professional master thesis – ITA, Instituto Tecnológico de Aeronáutica, São José dos Campos, SP, Brasil, 2009.
- NIEDERAUER DE OLIVEIRA, G. **Metodologia para Cálculo de Ruído Externo de Aeronaves**. Professional master thesis – ITA, Instituto Tecnológico de Aeronáutica, São José dos Campos, SP, Brasil, 2005.
- OLSEN, W. A. & FRIEDMAN, R. **Jet Noise From Coaxial Nozzles Over a Wide Range of Geometric and Flow Parameters**. AIAA Paper No. 74-43, Jan. 1974
- PIRK, ROGÉRIO. **Acústica e Vibroacústica**. São Jose dos Campos: ITA, 2003
- RIENSTRA, S.W. & HIRSCHBERG. **An Introduction to Acoustics**.
- RUSHWALD, IRA. **Boeing Airport Noise Symposium**, San Diego, 2002
- SANTOS, GUSTAVO DE FIORI DOS. **A Methodology for noise prediction of turbofan engines**. Doctor thesis – ITA, Instituto Tecnológico de Aeronáutica, São José dos Campos, SP, Brasil, 2006
- SCHMID, MICHAEL. **Entwicklung eines rogrammoduls zurPrognose des Lärms von Strahltriebwerken im Flugzeugvorentwurf**, 2001
- SCHMID, MICHAEL **Noise Applet**. Available in : <http://www.ilr.tu-berlin.de/LB/fed/Applets/applets/noise/noise.htm>, 2007
- SENGPIEL, E. **Calculation: absorption of sound by atmospheric air**. Available in: <http://www.sengpielaudio.com/calculator-air.htm>.
- SENGPIEL, E. **Conversion of sones-phone loudness level sone phon dBA dB sone dBA calculator fan noise**. Available in: <http://www.sengpielaudio.com/calculatorSonephon.htm>
- SMITH, MICHAEL J. T. **Aircraft Noise**, Cambridge, 1989
- STONE, J. R. **NASA TM X-71618 Interim Prediction Method for Jet Noise**, 1974
- WOLFE, J. **dB: What is a decibel**. Available in: <http://www.phys.unsw.edu.au/jw/dB.html>
- WIKIPEDIA **Doppler effect**. Available in: http://en.wikipedia.org/wiki/Doppler_effect, 2009

5. RESPONSIBILITY NOTICE

The author is the only responsible for the material included in this paper.